Anisotropic modeling of elastic wave velocities evolution In deformed shales

Joël Sarout and Yves Guéguen

Ecole Normale Supérieure – Department of Earth-Atmosphere-Ocean Sciences

CNRS – Geology Laboratory – UMR 8538

outline

- **Motivation:** Radioactive waste disposal in geologic layer (Callovo-Oxfordian shale)

- **Objectives and methodology**

- **Laboratory Experiments:** Elastic wave velocity measurements (ultrasonic frequency) under triaxial stresses on dry rocks

- **Effective Medium Modelling:** Intrinsic + microstructural anisotropies and prediction of fluid-saturated rock elastic properties

- **Conclusions and perspectives**

Radioactive waste disposal in shale layer

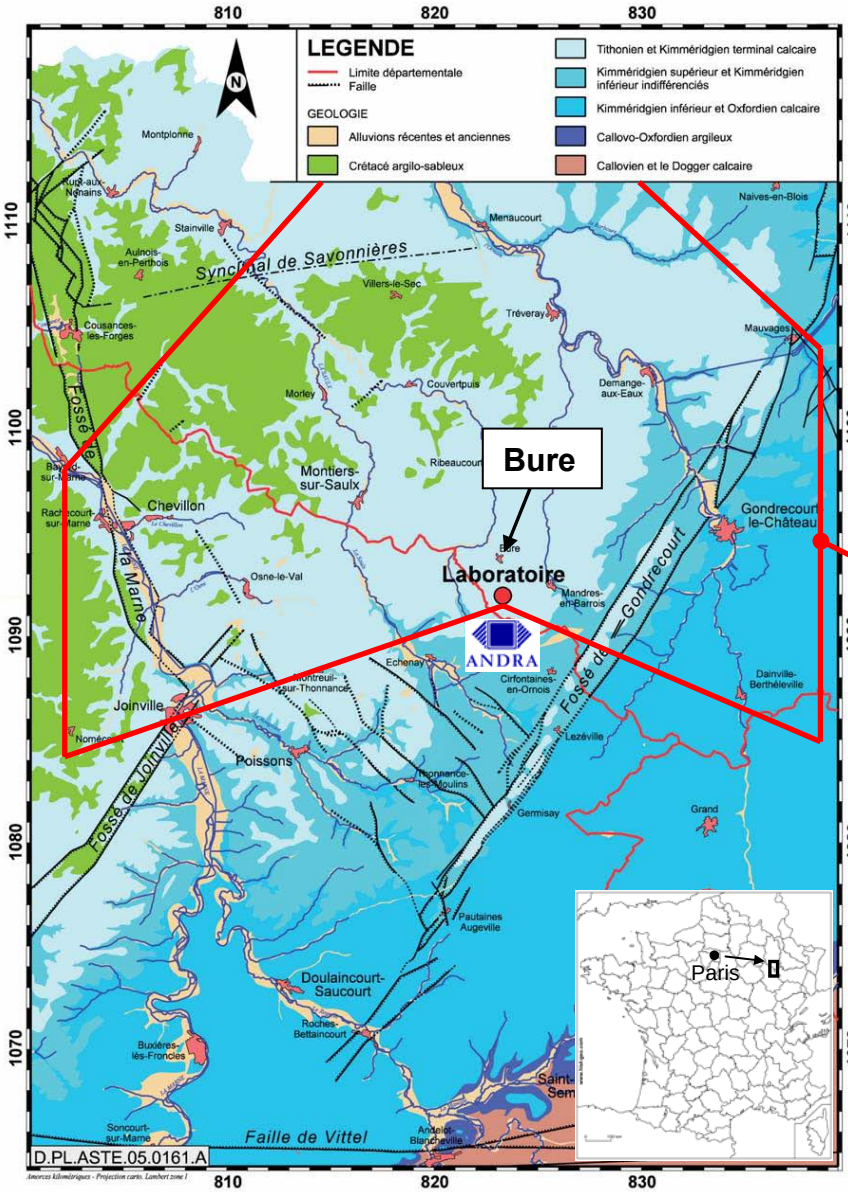

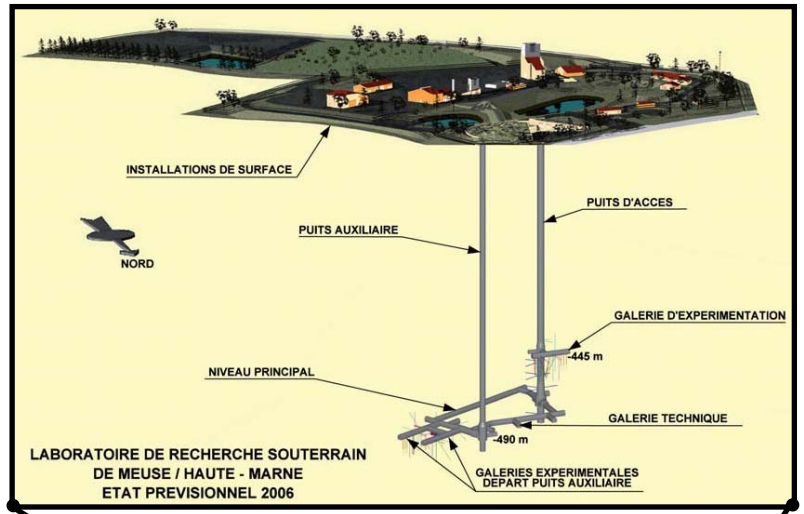

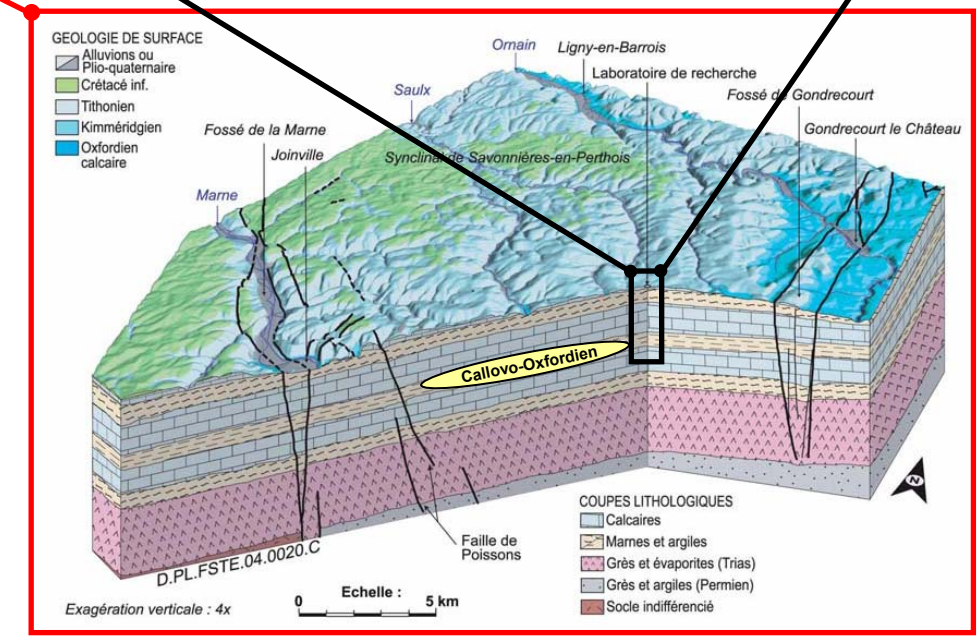

ANDRA Research Outcomes - 2005

Callovo-oxfordian shale

Microstructural Qualitative Analysis

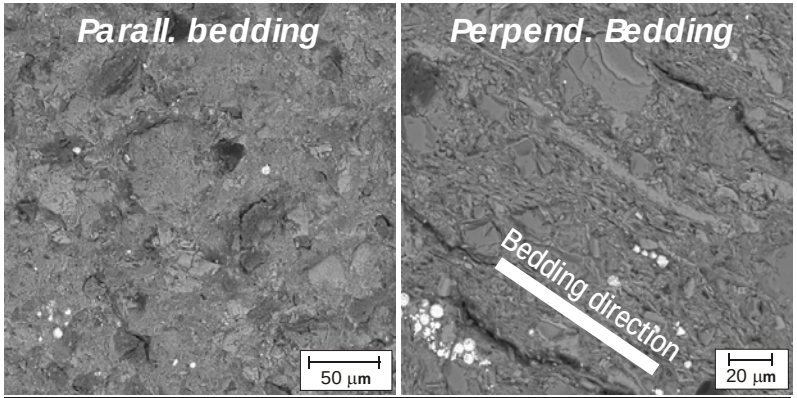

SCALE 0 $L = 10^{-9}$-10^{-8} m	Clay Platelets Superficial negative charges
SCALE 1 $L = 10^{-7}$-10^{-6} m	Clay Particule Adsorbed water
SCALE 2 $L = 10^{-5}$-10^{-4} m	± Ordered Clay Particules Microporosity MICROSCOPIC SCALE
SCALE 3 $L = 10^{-4}$-10^{-3} m	Shale: Composite material Clastic Inclusions Interfacial porosity Free water MACROSCOPIC SCALE

ANDRA Research Outcomes - 2005

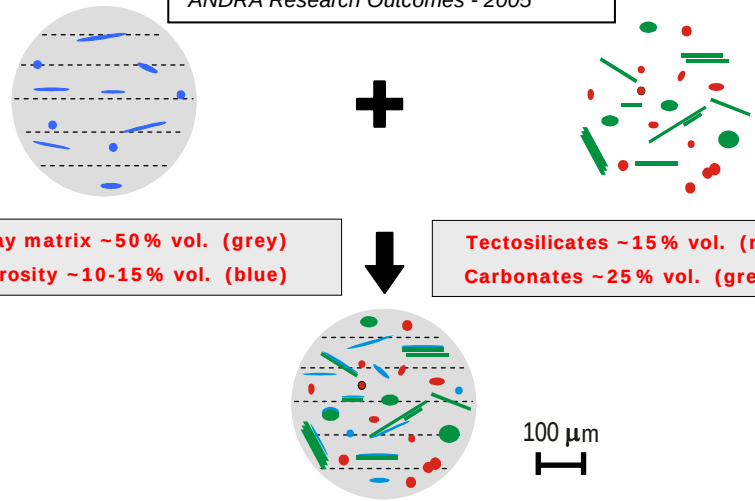

Ambiant Conditions Data

Elastic wave velocity data:

S-wave ~ 1.3 à 2 $km.s^{-1}$

P-wave ~ 2.4 à 3.7 $km.s^{-1}$

Gasc et al. (1999), Zamora et al. (2003)

Transverse Isotropy (5 elastic parameters)

P-wave anisotropy ~ 20-40%

Zamora et al. (2003), David et al. (2004)

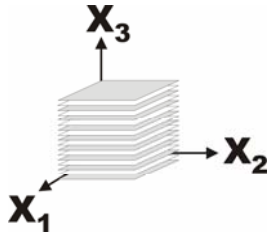

objectives and methodology

Callovo-Oxfordian Shale

Possible Causes of Anisotropy ??

- Intrinsic
  - Solide matrix:
    - clay matrix
    - Clastic inclusions
- Microstructural
  - Porosity :
    - Microcracks
    - Equant pores

Porosity : Geometry and Consequences

Permeability…

→ Sensitive to anisotropic porosity (crack-like pores, microcracks, interfacial porosity)

→ Stress-sensitive (microcracks closure)

Objectives

Explore micristructural changes under varying triaxial stresses

Methodology

Experimental tool:

Ultrasonic elastic wave velocity measurements

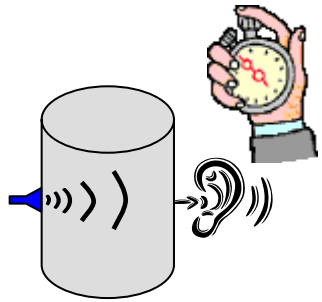

Theoretical tool:

Micromechanical modelling

Eshelby's inhomogeneity

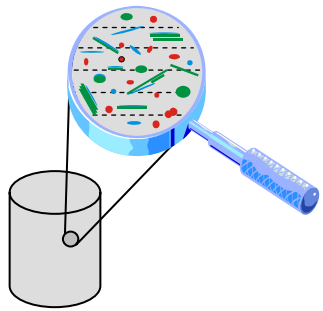

Experiments: ambiant conditions

Shale Specific Properties

- Very low permeability (10^{-20}-10^{-22} m^2)
- Sensitivity to acqueous fluids (hydration and osmotic swelling)

Samples Preparation

- Dry cutting
- Preserved samples (isolated cells) *or*
- Equilibrated in given air humidity conditions

Ambiant Conditions Data

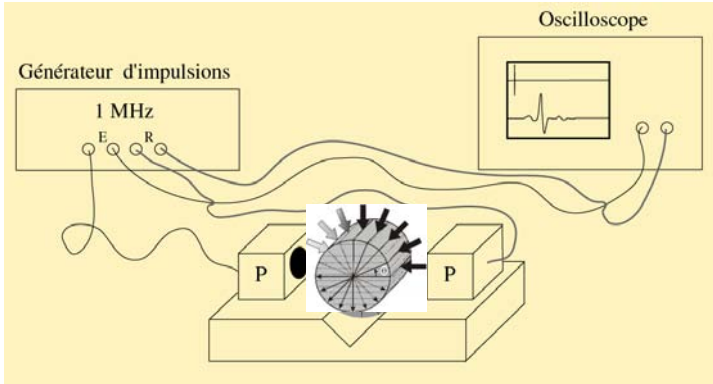

Université Cergy Pontoisse

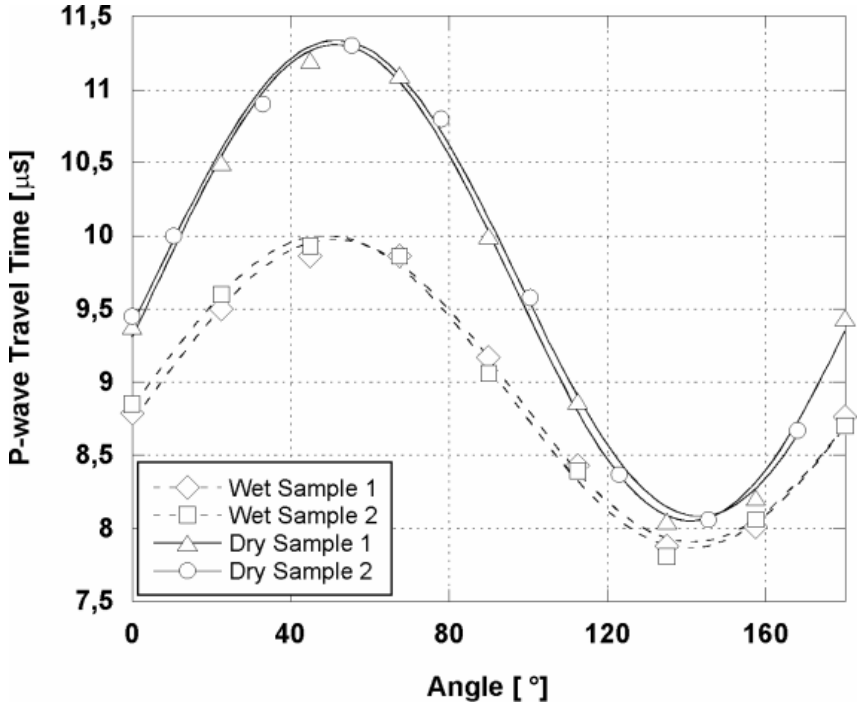

Experiments: Undrained triaxial deformation

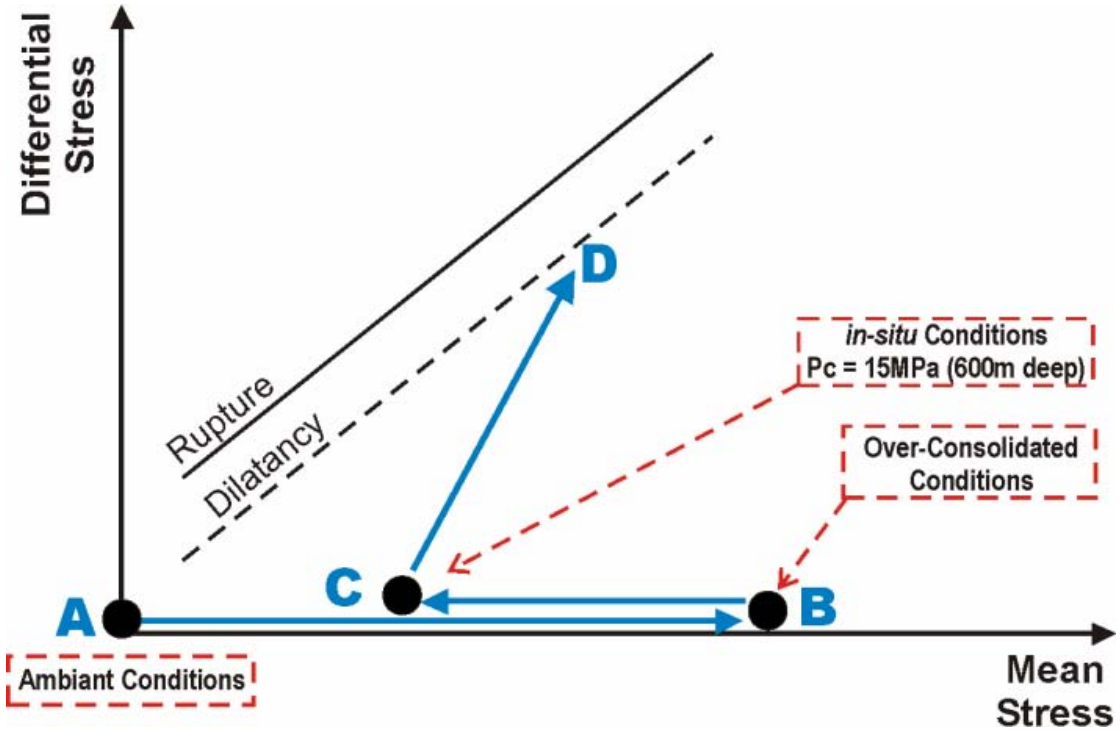

Exp. #	Sample	Loading	I.C.	Cycle P_c [MPa]	Cycle σ_{ax} [MPa]
I	MSE 101	Isotropic	Preserved	0-180-0	0
II	MSE 101	Isotropic	HR = 98%	0-200-0	0
III	MSE 101	Triaxial	105°C	0-55-15	0-91-0-103
IV	REP 2206	Triaxial	HR = 0%	0-55-11	0-88
V	MSE 101	Triaxial	Preserved	0-20-2-55-15	0-45-0-48
VI	MSE 101	Triaxial	HR = 98%	0-55-15	0-36-0-37

Experimental setup : triaxial cell

- **Samples:** Ø = 3-4 cm, L = 6-8 cm
- **Isotropic stress: P_c = 300 MPa**
- **Axial stress: σ_{ax} = 800 MPa**
- **Pore pressure: P_p = 100 MPa**
- **Direct measurements:** 16 transducers (strain gauges, piezoelectric ceramics), 2 external LVDTs, 10 pressure transducers
- **Automatic control:** in stress or in displacement (Labview™)
- **Data acquisition:** computerized (Labview™)

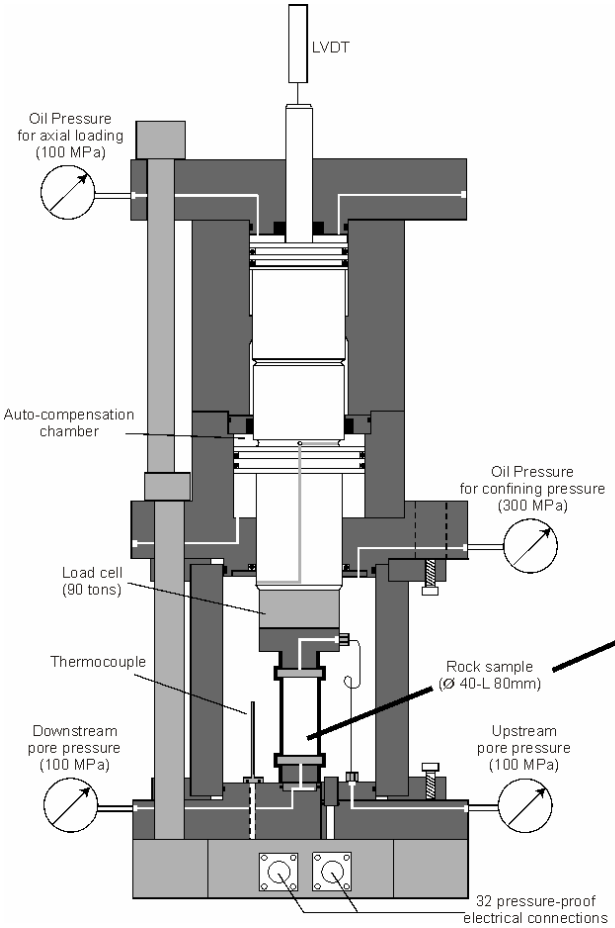

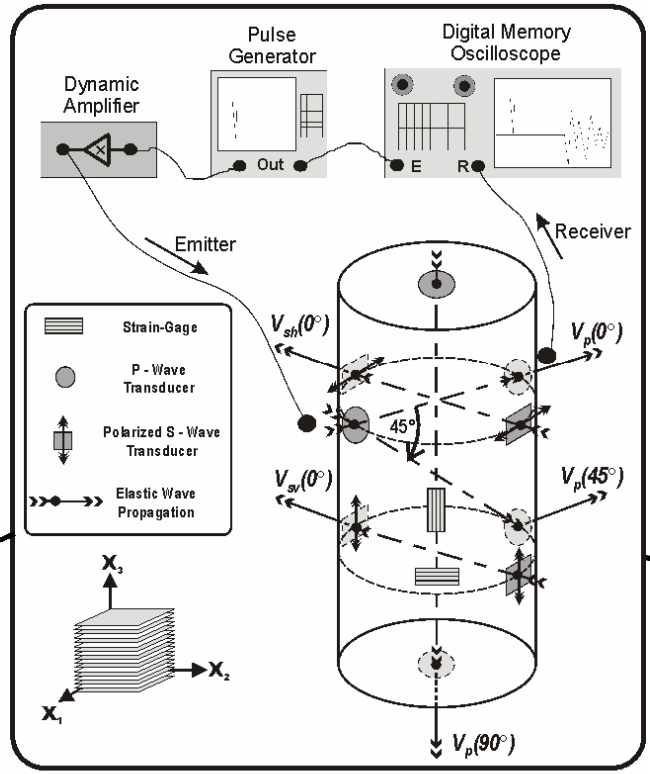

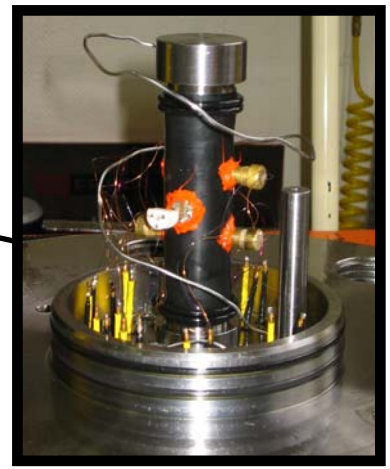

Experimental results: stress-strain data

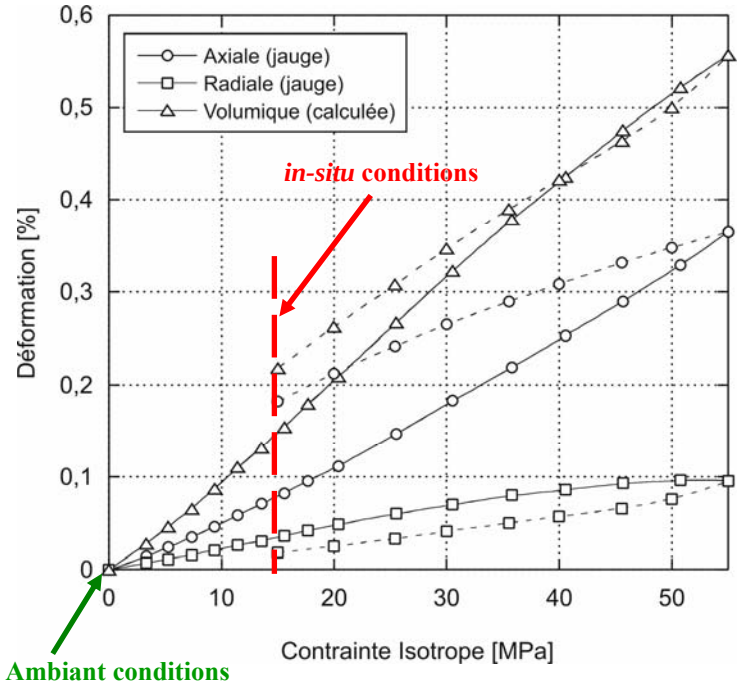

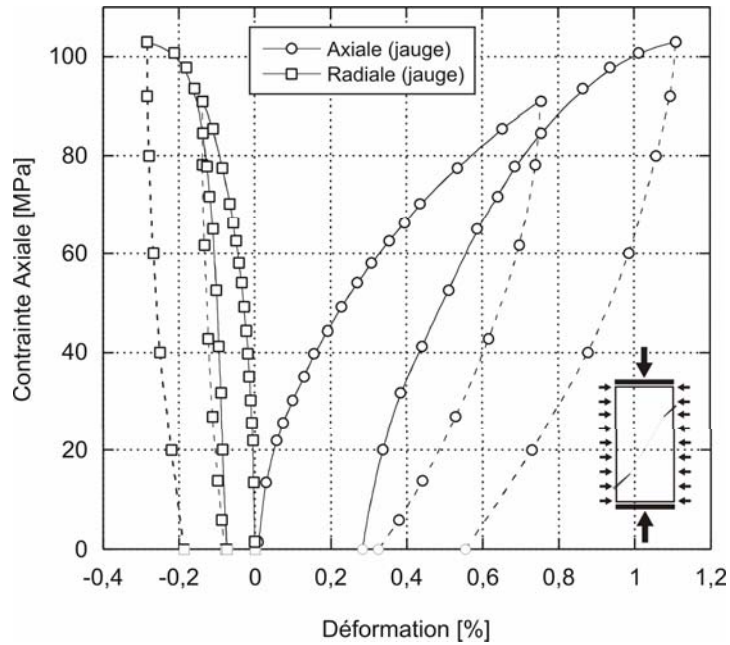

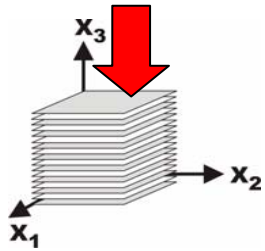

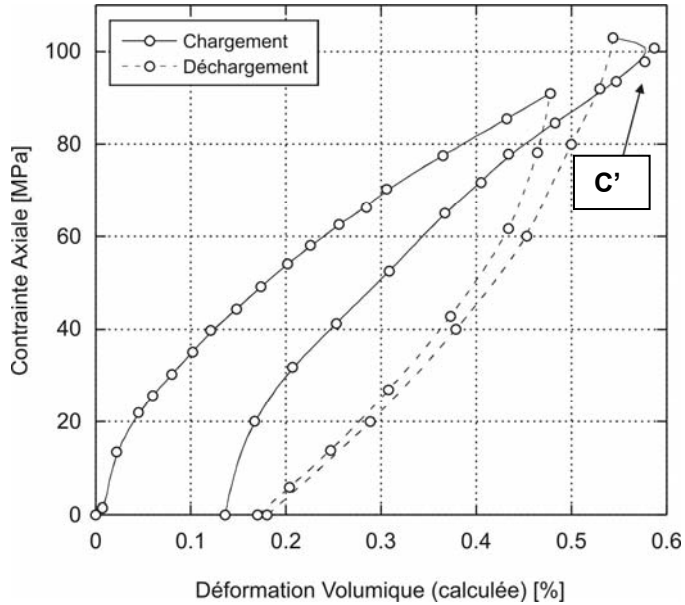

- **Anelastic and anisotropic strain under isotropic stress variations**
- **Static anisotropy increases with isotropic stress**
- **Irreversible strain under deviatoric stress increase applied ⊥ bedding plane**
- **Dilantancy threshold C' under deviatoric stress applied ⊥ bedding plane**
- **Shear plane rupture at ≅ 45°**
- $\varepsilon_{vol}^{iso} \cong 0.55\ \%$ **et** $\varepsilon_{vol}^{ax} \cong 0.6\ \%$

Experimental results: elastic wave velocities

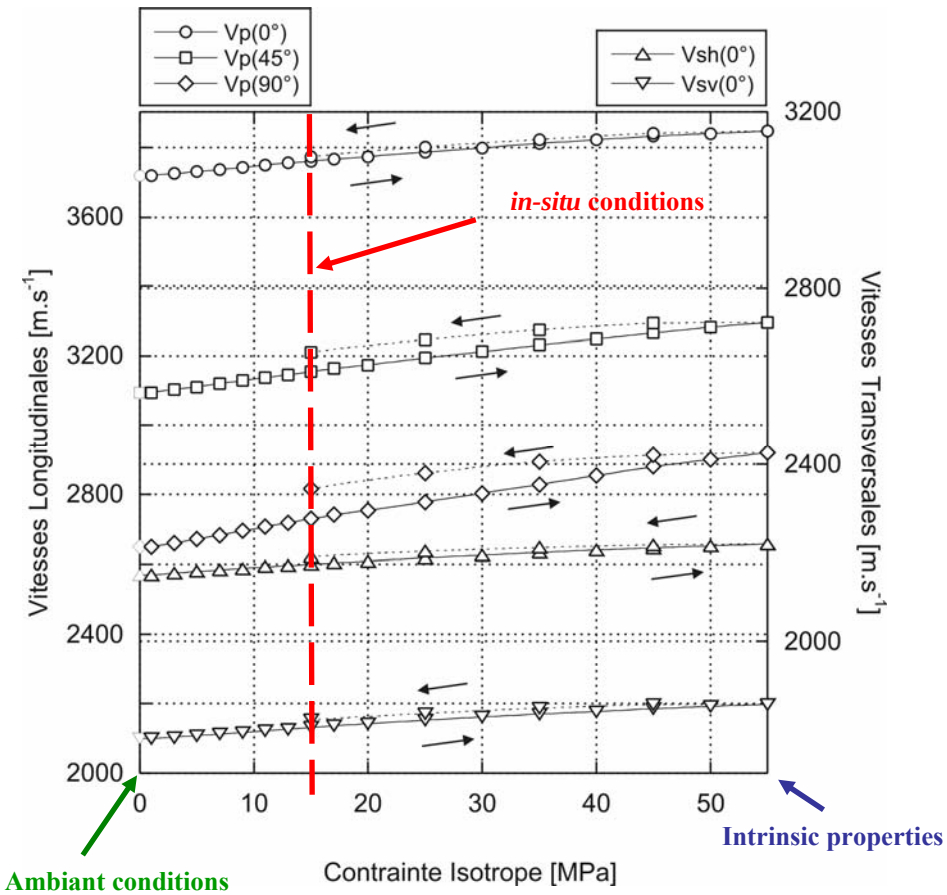

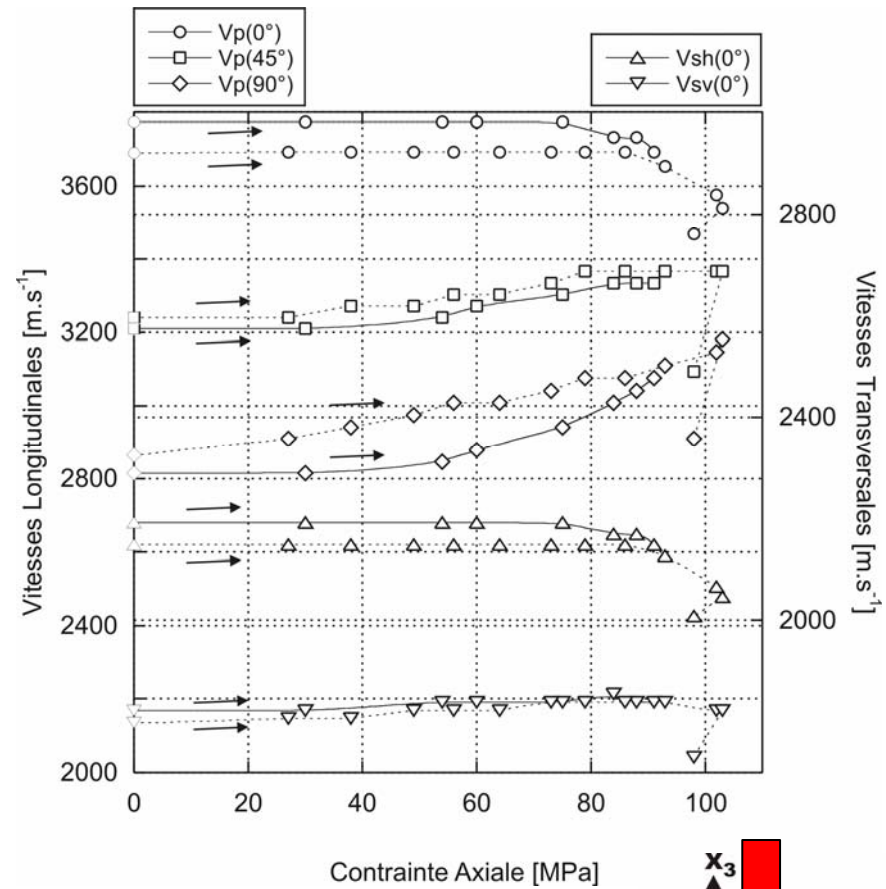

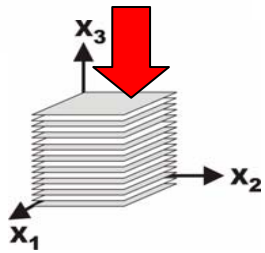

- All elastic wave velocities increase with isotropic stress
- $V_p(45°)$ and $V_p(90°)$ increasewith deviatoric stress applied ⊥ bedding plane
- $V_p(0°)$, $V_{SH}(0°)$ et $V_{SV}(0°)$ decrease with deviatoric stress applied ⊥ bedding plane
- $V_p(0°)$ et $V_{SH}(0°)$ rupture precursors

Elastic interpretation

Transversely Isotropic Elasticity

$$\sigma_{ij} = C_{ijkl}\ \varepsilon_{kl}$$

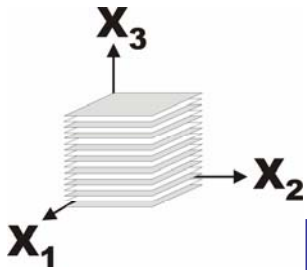

$$C_{ijkl} = \begin{bmatrix} C_{11} & C_{12} & C_{13} & 0 & 0 & 0 \\ C_{12} & C_{11} & C_{13} & 0 & 0 & 0 \\ C_{13} & C_{13} & C_{33} & 0 & 0 & 0 \\ 0 & 0 & 0 & C_{44} & 0 & 0 \\ 0 & 0 & 0 & 0 & C_{44} & 0 \\ 0 & 0 & 0 & 0 & 0 & C_{66} \end{bmatrix}$$

$$C_{12} = C_{11} - 2C_{66}$$

Measurements Inversion

$$C_{11} = \rho V_P^2\left(0^o\right) \qquad C_{33} = \rho V_P^2\left(90^o\right)$$

$$C_{44} = \rho V_{SV}^2\left(0^o\right) \qquad C_{66} = \rho V_{SH}^2\left(0^o\right)$$

$$C_{13} = -C_{44} + \sqrt{\left(C_{11} + C_{44} - 2\rho V_P^2\left(45^o\right)\right)\left(C_{33} + C_{44} - 2\rho V_P^2\left(45^o\right)\right)}$$

P-wave

$$\varepsilon = \frac{C_{11} - C_{33}}{2C_{33}}$$

S-wave

$$\gamma = \frac{C_{66} - C_{44}}{2C_{44}}$$

Anellipticity $\eta \propto \varepsilon - \delta$

$$\delta = \frac{\left(C_{13} + C_{44}\right)^2 - \left(C_{33} - C_{44}\right)^2}{2C_{33}\left(C_{33} - C_{44}\right)}$$

Thomsen (1986)

evolution of elastic anisotropy

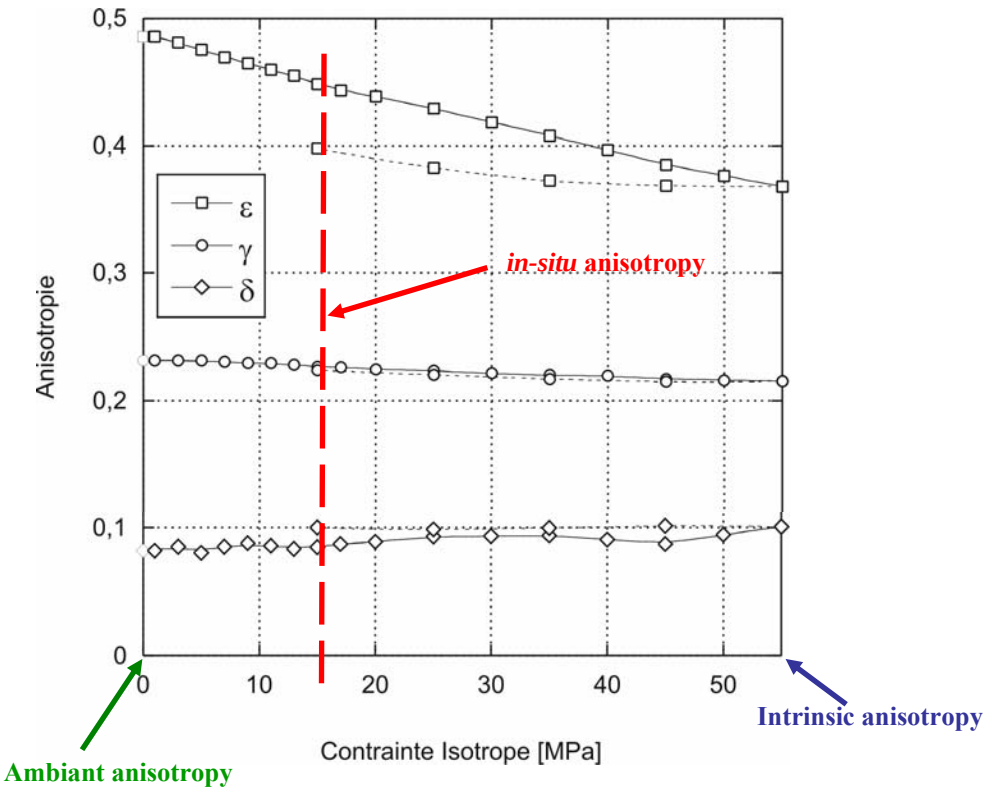

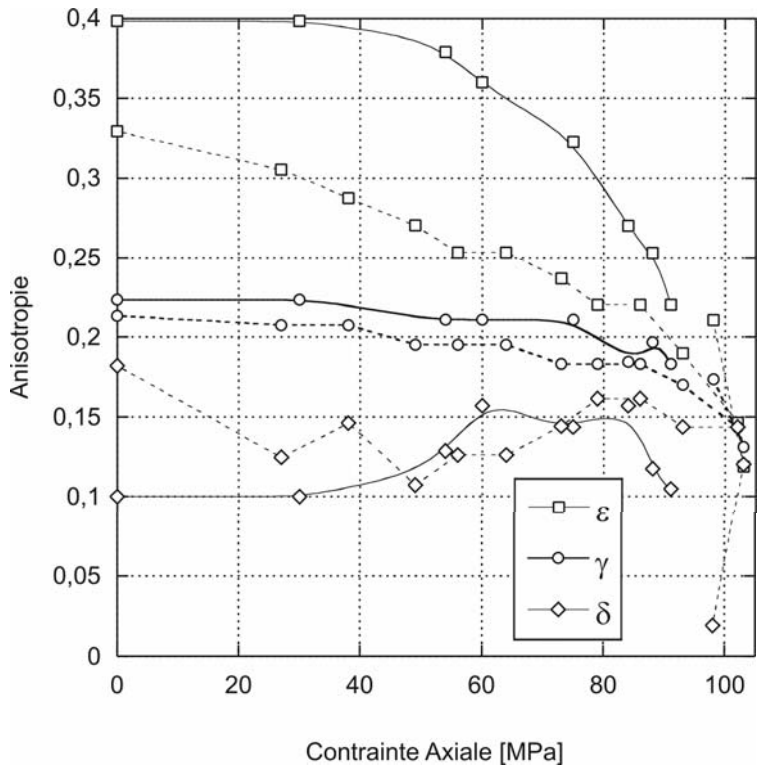

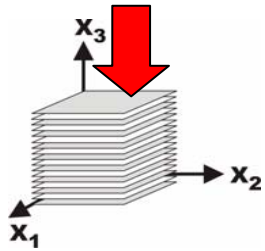

- **Elastic anisotropy decreases with isotropic stress**
- **Elastic anisotropy decreases with deviatoric stress applied ⊥ bedding plane**
- **Intrinsic elastic anisotropy ≠ 0**

Anisotropy becomes a tool for accurate microstructural properties identification

microcracks evolution under varying stress

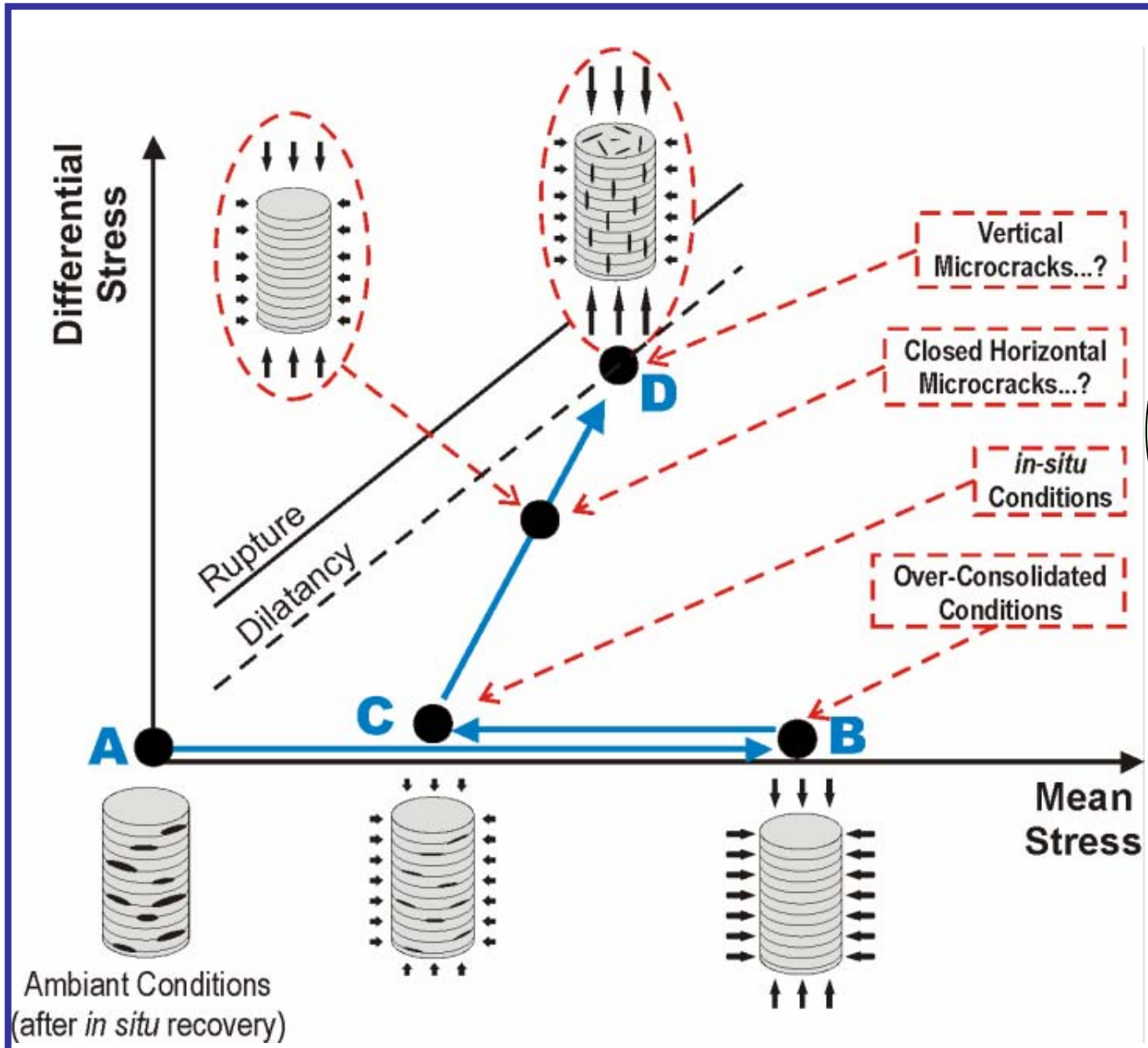

Effective medium model

=

Transversely isotropic solid (Intrinsic anisotropy)

+

Transversely isotropic distribution of pores/microcracks (geometry and orientation)

Micromechanical modelling: Eshelby's problem

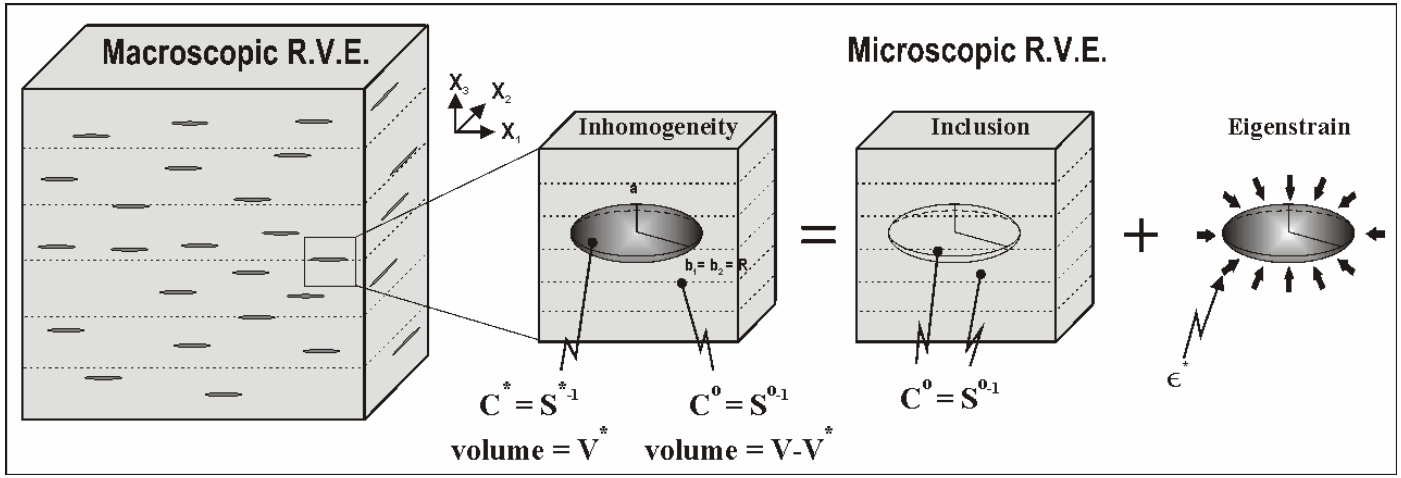

Eshelby (1957)

Compliant Porosity ⇔ Source of Strain

$$\varepsilon = \varepsilon^o + \Delta\varepsilon = \left(S^o + \Delta S\right) : \sigma$$

$$\Delta S = \frac{V^*}{V}\left[\left(S^* - S^o\right)^{-1} + C^o : \left(J - s\right)\right]^{-1}$$

s = Eshelby's Tensor

Transversely Isotropic Solid

+

Oblate Spheroid: ξ = a/R

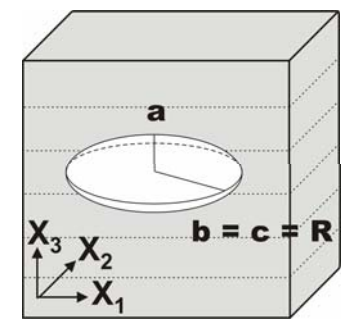

Lin & Mura (1973), Whiters (1989)

Microstructural Parameters

Porosity ϕ, Aspect ratio ξ, Fluid Incompressibility $\mathbf{K_f}$ … and $\mathbf{C^o}$

Theoretical predictions

Co = High Pressure Moduli

C11o = 34.5 GPa

C33o = 19.9 GPa

C44o = 8 GPa

C66o = 11.5 GPa

C13o = 5.6 GPa

Parameters	Ref. Value
ξ	1/100
ϕ	0.5 %

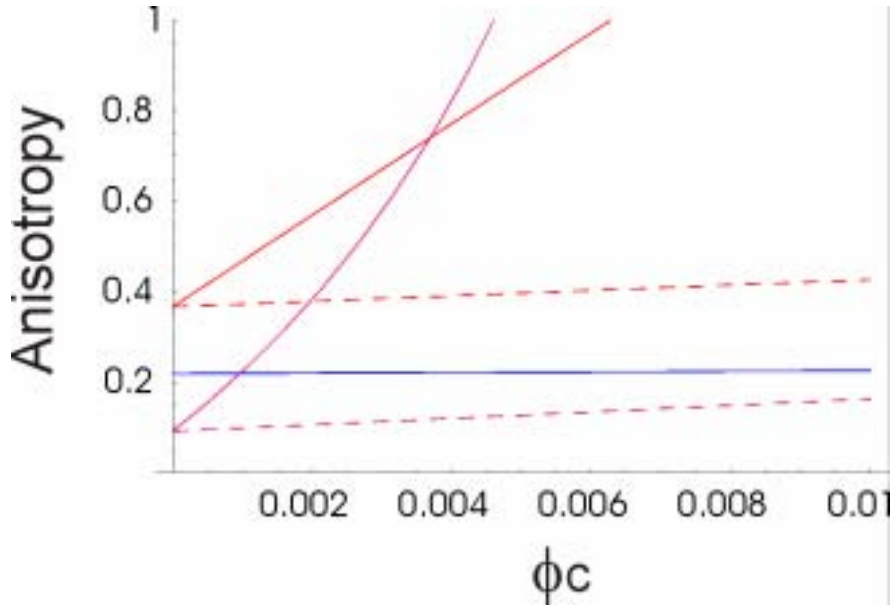

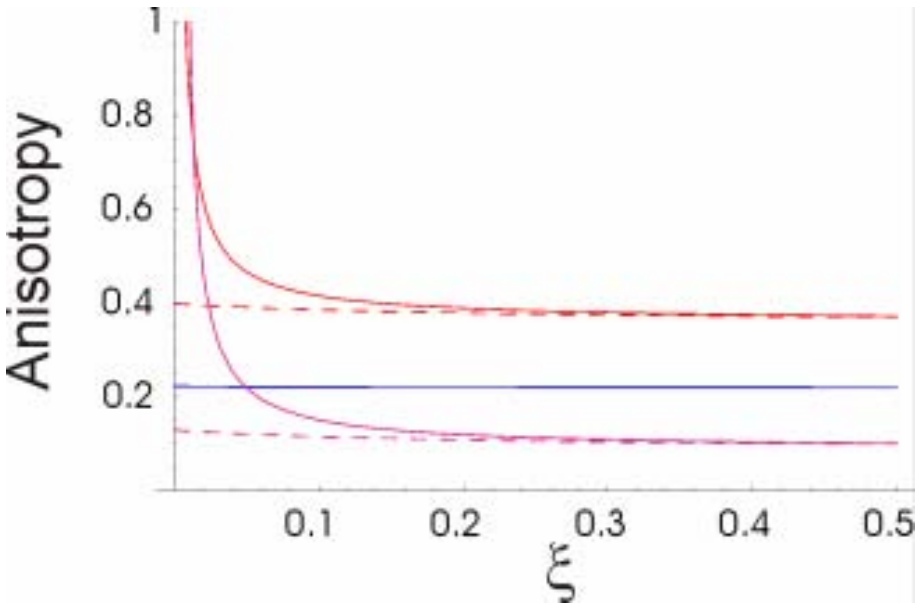

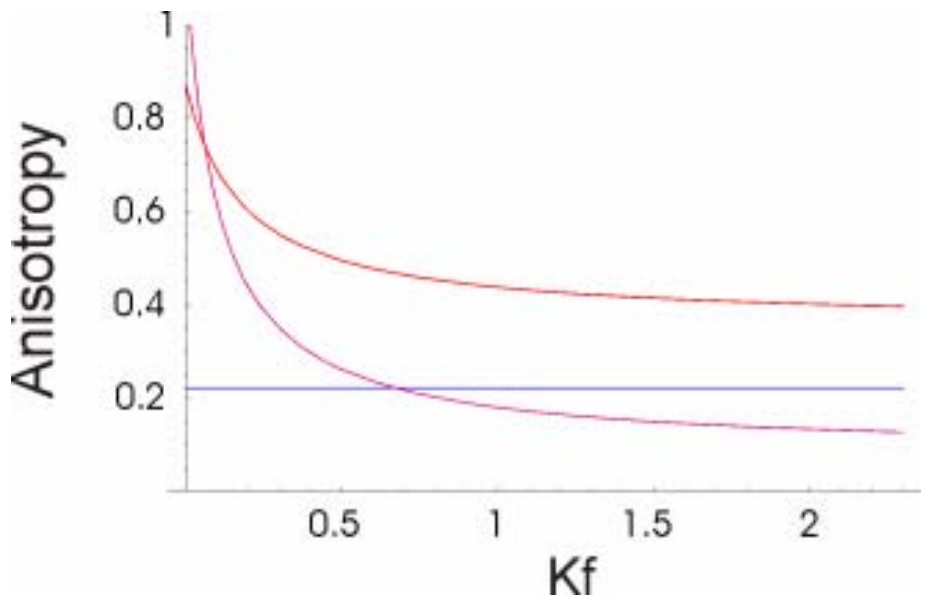

Experiments vs theory (1)

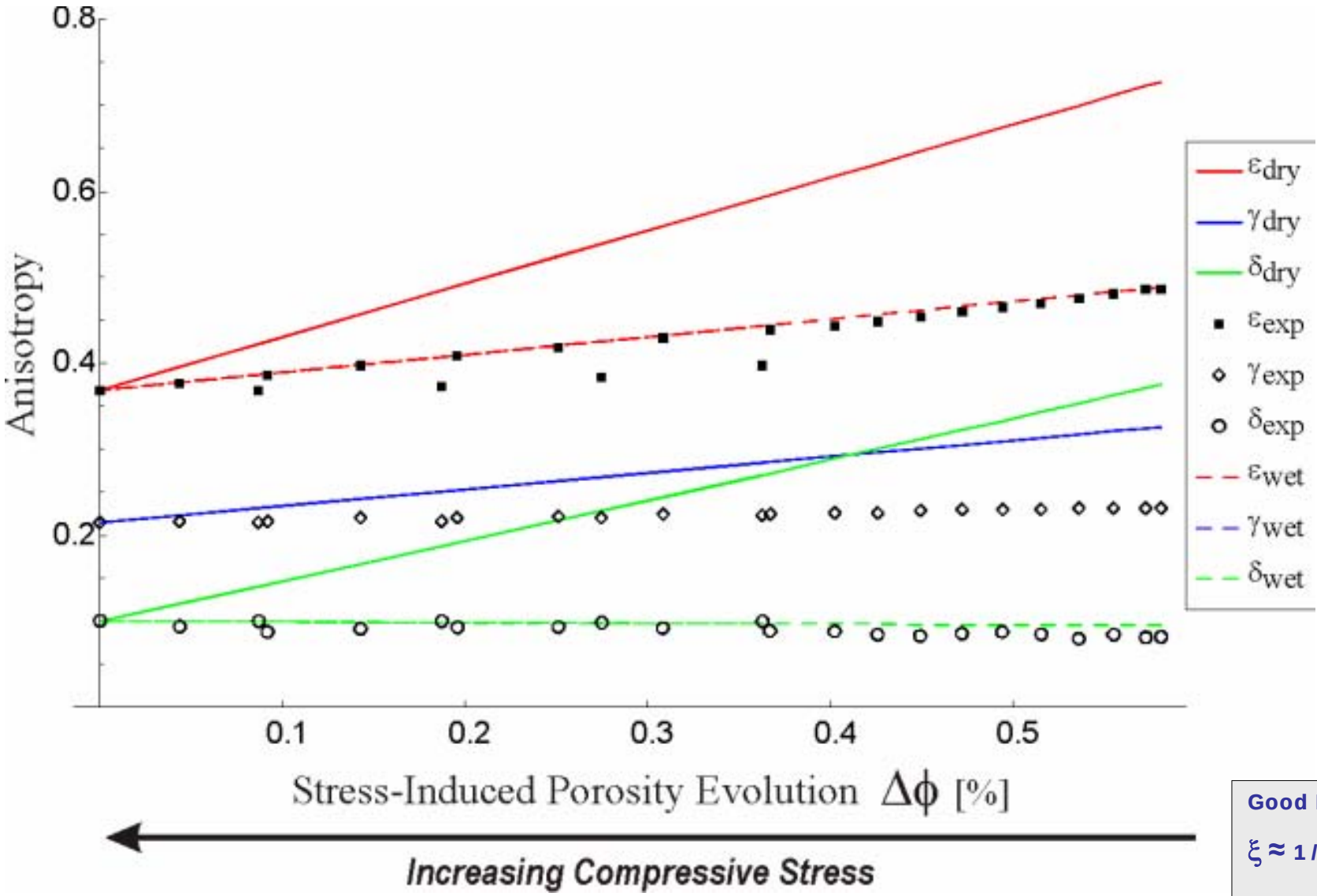

Good Fit for:

$\xi \approx 1/100$

$K_f \approx 0.5$ GPa

Experiments vs theory (2)

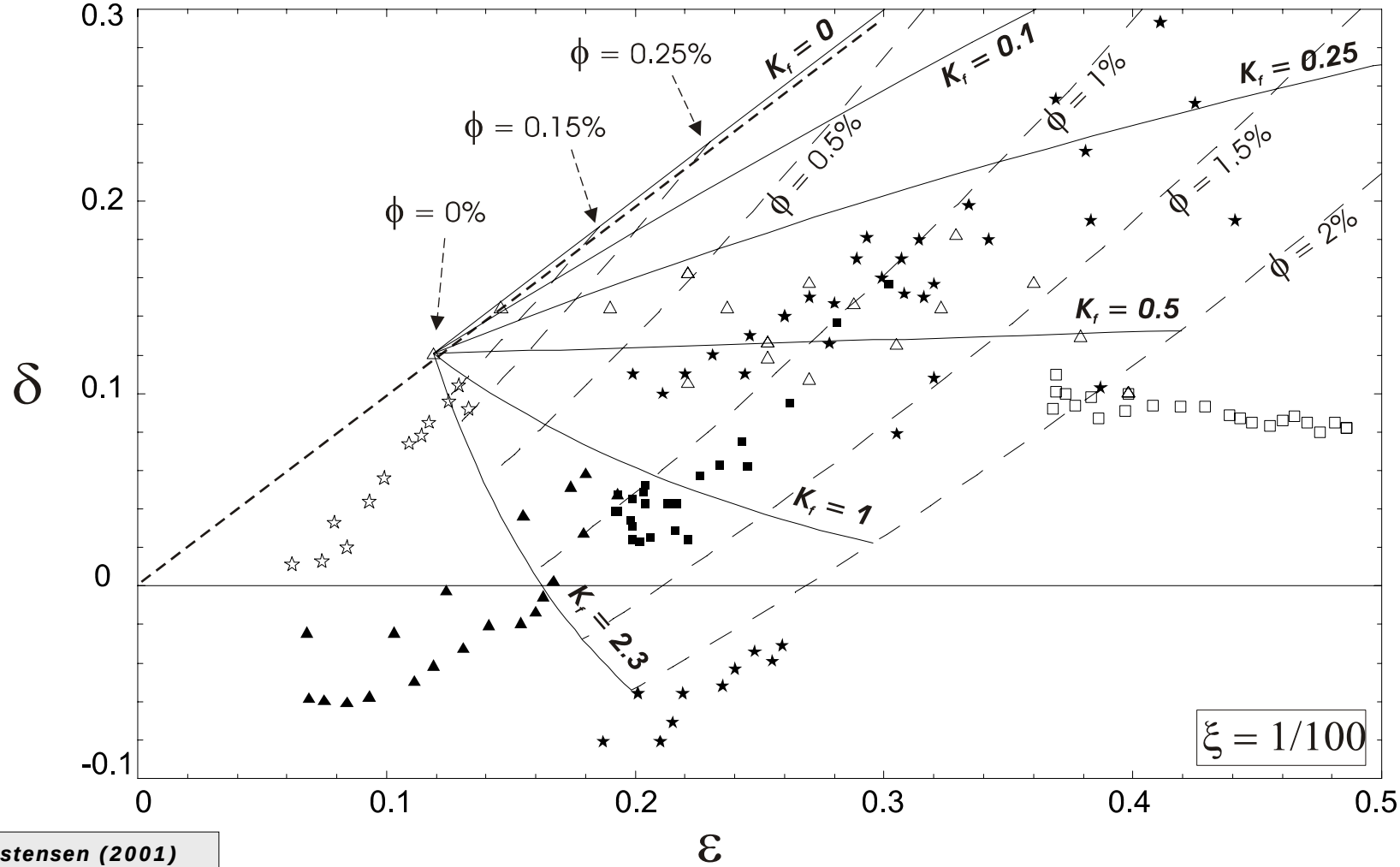

Stanley & Christensen (2001)
Hornby (1998)
Vernik & Liu (1997)
Johnston & Christensen (1995)
Lo, Coyner & Toksöz (1986)
Jones & Wang (1981)

□ Conf Dry	■ Conf Wet	☆ Conf Dry
△ Dev Dry	▲ Dev Wet	★ Conf Wet

Conclusions

Callovo-Oxfordian shale backround rock is transversely isotropic

+

Crack-like pores / microcracks are more or less aligned with the rock bedding plane

Mean aspect ratio $\approx$ 1 / 100

↓

Transversely isotropic effective properties

Elastic data:

Wet shale anisotropy < Dry shale anisotropy at ambiant conditions

Wet shale elastically stiffer than dry shale at ambiant conditions

Elastic anisotropy ε, γ and δ decrease with increasing isotropic stress in dry shale

Modeling:

Elastic shear anisotropy γ should be insensitive to fluid incompressibility Kf

Perspectives…

Experimental Perspectives

Perform higher confining pressure experiments on dry shale samples

⇒ assess intrinsic elastic properties

Perform experiments on shale samples cored in different directions w.r.t. bedding plane

Theoretical Perspectives

Micromechanical model limited to horizontal oblate spheroids

↓

Approximate shale intrinsic elastic properties by means of an energetically equivalent isotropic solid

↓

Extrapolate ultrasonic laboratory data to low frequency range using Brown & Korringa poroelastic relations

Annexe I : ambiant conditions data

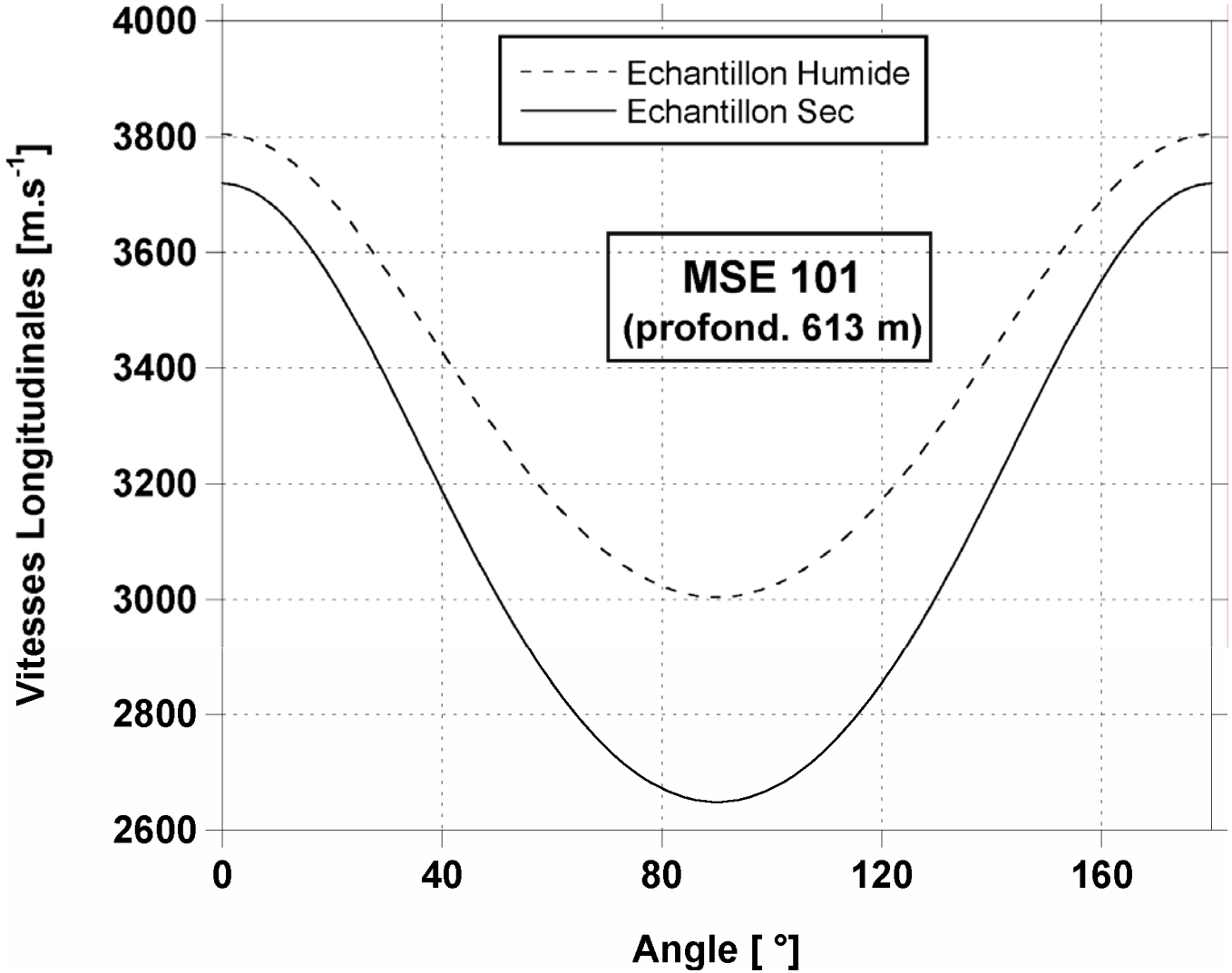

appendix II : components of eshelby's tensor

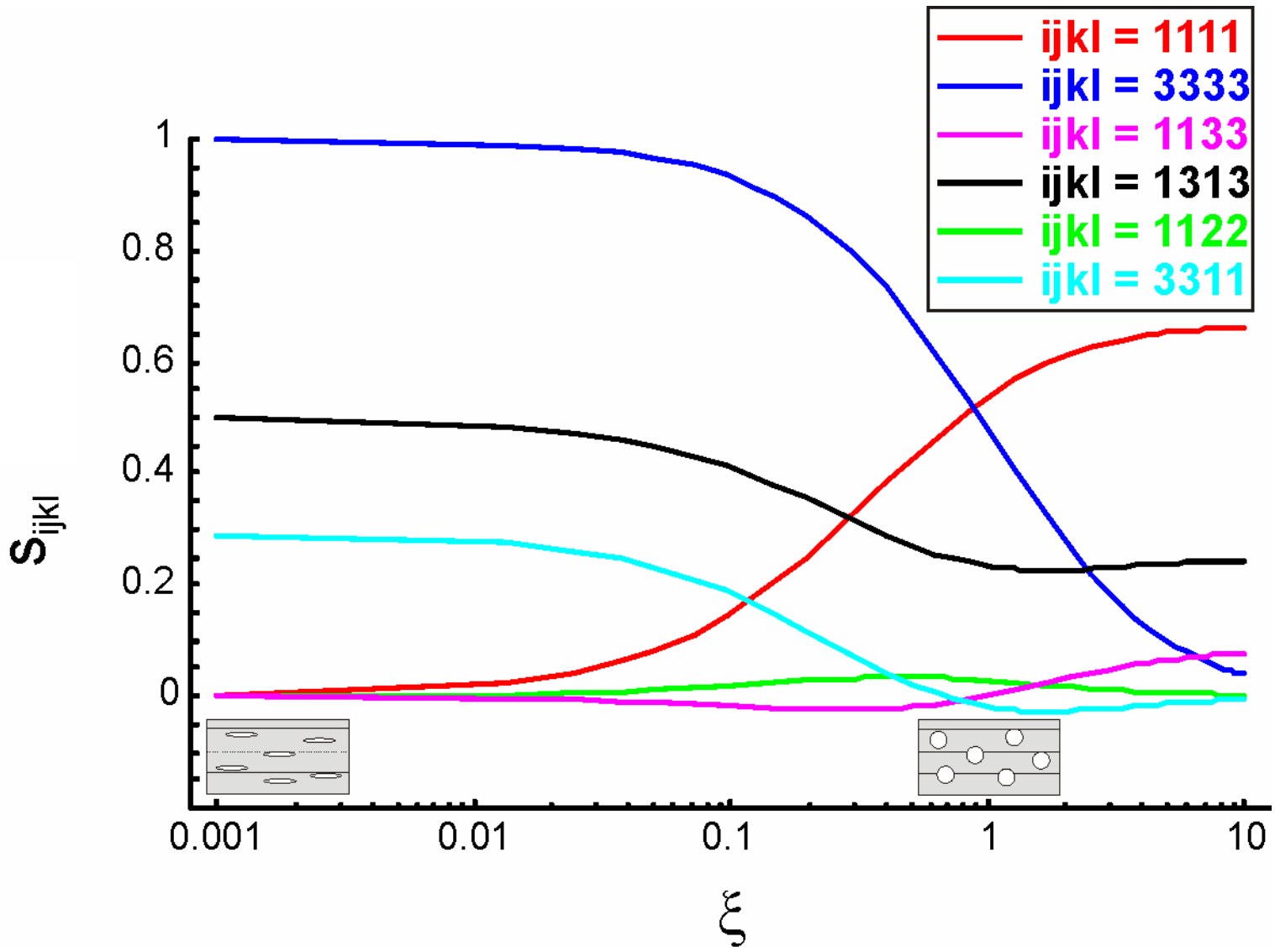

appendix III : water and clays

Pore Water

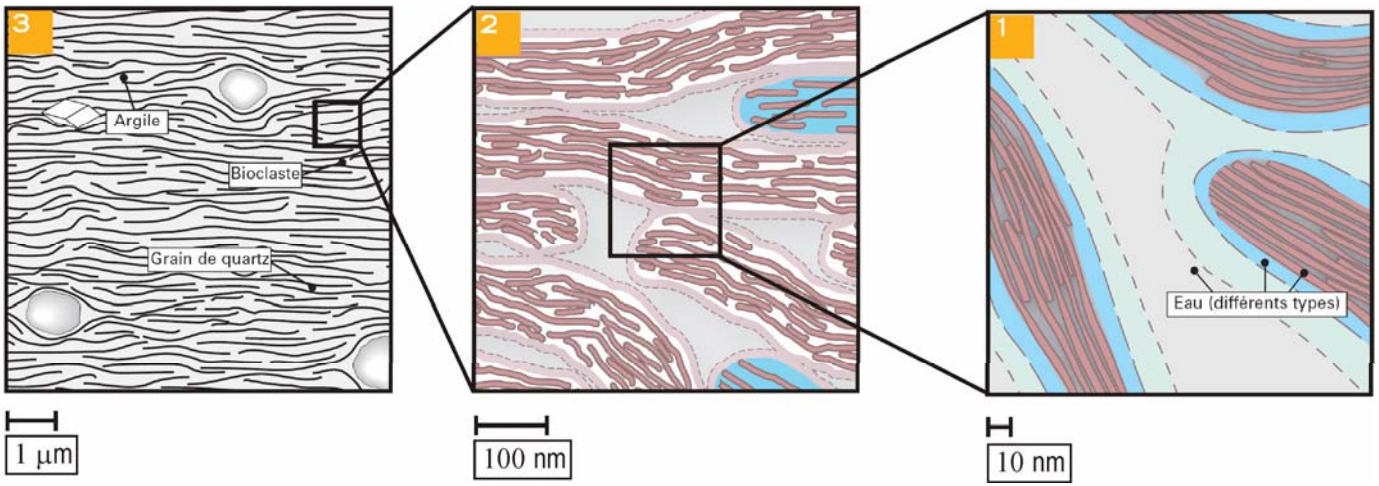

ANDRA Research Outcomes - 2005